AstroPIC: Near-Infrared photonic integrated circuit coronagraph architecture for the Habitable Worlds Observatory

Dan Sirbu[*], Ruslan Belikov[1], Kevin Fogarty[1], Carson Valdez[2], Zhanghao Sun[2], Annie Kroo[2], Olav Solgaard[2], David A. B. Miller [2], Olivier Guyon [3]

[1]NASA Ames Research Center, Moffett Field, Mountain View, CA

[2]Electrical & Computer Engineering, Stanford University, Stanford, CA [3]Subaru Telescope - NAOJ, Hilo, HI / University of Arizona, Tucson, AZ

ABSTRACT

The Habitable Worlds Observatory (HWO) is the leading recommendation of the Astro2020 decadal survey. The HWO flagship, to be launched in the early 2040s, will directly survey 100 of the nearest stellar systems and their habitable zones with the goal of detecting and spectroscopically characterizing 25 potentially "Earth-like planets" (or "Exo-Earths"). Photonic-based technologies can substantially improve technical and science margins by improving coronagraphic efficiency for HWO.

We present the architecture of a photonic-integrated circuit (PIC)-based coronagraph ("AstroPIC"), currently being studied as a near-infrared channel coronagraph that can be adopted as part of a suite of coronagraphs that could be deployed on the HWO. The PIC architecture miniaturizes a traditional coronagraph reducing the mass and volume of the coronagraph while providing an avenue to simply enhance the functionality, bandwidth coverage, and exoplanet yield of HWO by adopting a Mach-Zehnder Interferometric (MZI) mesh for photonic nulling. In this architecture we consider two cases: (1) a hybrid AstroPIC using a small number of modes (16-25) can still enhance exoplanet yields through complementary coronagraphic sensitivities to a traditional coronagraph, and (2) a full photonic chip AstroPIC that uses larger number of modes (400+) that can be operated as a stand-alone coronagraph that approaches the optimal coronagraph performance limit. We summarize recent experiments carried out at the Stanford photonic teststand which demonstrate key coronagraphic functionality including: (1) 1e-7 contrast (70 dB nulling) achieved with a simple PIC consisting of a 4-MZI mesh, (2) 8e-9 contrast (81 dB nulling) achieved with 6-MZI elements, and (3) a free-space coupling on chip of a beam demonstrating coronagraphic nulling and coronagraphic throughput of an off-axis source. We discuss the recent AstroPIC Cycle-1 tape-out which will enable additional coronagraphic demonstrations including deeper nulling and scaling to larger numbers of modes initiating a technology development process to mature PIC-based coronagraphy for inclusion into HWO.

Keywords: Astrophotonics, Photonic Integrated Circuits, Exoplanets, Coronagraphy, High-Contrast Imaging, Wavefront Control, Habitable Worlds Observatory, Near-Infrared Channel

1. INTRODUCTION

The Habitable Worlds Observatory (HWO) is the leading recommendation of the Astro2020 decadal survey.[1] The HWO flagship, to be launched in the early 2040s, will directly survey 100 of the nearest stellar systems and their habitable zones with the goal of detecting and spectroscopically characterizing 25 potentially "Earth-like planets" (or "Exo-Earths"). The HWO telescope will feature a segmented aperture with at least a 6-m inscribed diameter and a science instrument (called a "coronagraph") that will suppress starlight by ten orders of magnitude to reveal the reflected light from orbiting dim, rocky exoplanets at the small angular separations that span the host star's habitable zone. Photonic-based technologies can substantially improve technical and science margins by improving coronagraphic efficiency for HWO.
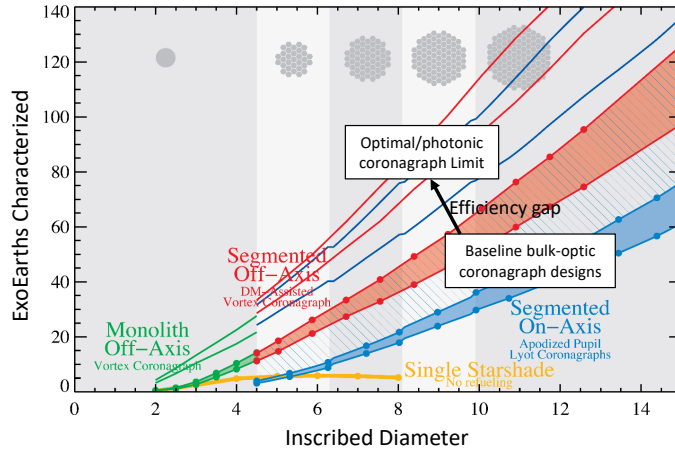
---

*email: dan.sirbu@nasa.gov

Figure 1: Characterized Exo-Earths estimate (i.e., mission "science yield") as a function of telescope diameter for current baseline "bulk-optic" or "traditional" coronagraph designs considered by Astro2020. Shown also are the theoretical limits obtainable using an optimal coronagraph that represent a design implementable through a photonic integrated chip coronagraph (from,[2] with figure by C. Stark). Number of Exo-Earths characterized by HWO for a photonic coronagraph increases from 25 to over 50 for a 6-m inscribed diameter aperture.

As shown in Figure 1, current baseline coronagraph designs are inefficient compared to the theoretical, fundamental limits possible with optimal coronagraph designs. The difference between state-of-the-art and future optimal coronagraphs that are theoretically possible represents an "efficiency gap" that has been recognized by the NASA Exoplanet Exploration Program and is now part of Astrophysics Directorate's "technology gap list".[3] Closing this efficiency gap through early instrument development and new technologies can potentially more than double the expected number of characterized exoplanets (i.e., mission "science yield") from the HWO coronagraph instrument and introduce a significant margin to mitigate risks for the mission, such as lower-than-expected Earth-like planet occurrence ($\oplus$), and unexpected challenges for both telescope stability and mission development. In recognition of the potential for improved mission efficiency, the second top recommendation of the Astro2020 decadal survey was the start of a "Great Observatory Technology Maturation Program" (GOMAP) prior to the start of Phase A activities for HWO with a greater scope and depth commensurate with HWO's scientific requirements.

Photonic Integrated Circuits (PICs) are an emerging technology with a wide variety of applications to astronomical instrumentation ("astrophotonics"[4]) and hold the potential to significantly improve the performance, reduce volume and mass, and enhance functionality. PIC development kits for different substrate technologies (e.g., silicon, silicon nitride, glass) and are now being offered by commercial foundries enabling low-cost iteration through custom-designed photonic chips for novel applications and enhanced functionality.

In this paper, we present the architecture of a photonic-integrated circuit (PIC)-based coronagraph ("AstroPIC") as a a near-infrared channel coronagraph that can be adopted as part of a suite of coronagraph for HWO. The PIC architecture miniaturizes a traditional coronagraph reducing the mass and volume of the coronagraph while providing an avenue to simply enhance the functionality, bandwidth coverage, and exoplanet yield of HWO. This is a flexible and extensible architecture that is fully compatible with a wide variety of possible HWO apertures (including both on-axis and off-axis), and can be tailored to specific observations through reconfigurations based on the astrophysical properties of the current target star (e.g., stellar diameter, habitable zone separation, etc.).

In this architecture we consider two cases: (1) a "hybrid" AstroPIC which uses a small number of modes (16-25) that can still enhance the science yields through complementary coronagraphic sensitivities to a traditional coronagraph, and (2) a "full photonic chip" AstroPIC that uses larger number of modes (400+) that can be operated as a stand-alone coronagraph and is shown to approach the optimal coronagraph performance limit. The hybrid AstroPIC configuration could be matured relatively rapidly with a small number of modes being close to

current manufacturing capabilities (though still requiring relevant experimental demonstrations) and would entail a PIC operating simultaneously with a traditional coronagraph and utilizing the light that is traditionally rejected by the coronagraph for enhanced exoplanet science gains. Alternatively, the full photonic chip AstroPIC would require significant technology maturation to scale to a large number of modes and miniaturize the coronagraph instrument.

Currently, a silicon substrate platform is the most mature based on developments from the telecom industry with an overlap in observation capabilities in C-band (centered at 1.55 um) with the HWO near-infrared (NIR) channel requirements (currently envisioned as 1-1.8 um); however, silicon nitride platforms are quickly developing and hold the potential to operate in visible bands down to 400 nm. A NIR channel AstroPIC leverages key characteristics of a PIC coronagraph such as its aggressive inner working which is complementary to traditional baselined coronagraphs. Key performance metrics required to enable a PIC coronagraph are deep photonic nulling (at 10^{-10} contrast), aggressive inner working angles, and increased outer working angles, high coronagraphic throughput, robustness to disturbances, and broad bandwidth. All of these performance indicators should be demonstrated and traded-off as part of a concerted technology maturation program. Due to their small mass and volume, it is simple to add more PIC channels to enable wider band characterization.

This paper has a central goal of providing an overview of the AstroPIC project and its architecture, summarizing recent experimental results, and the Cycle-1 prototype. In Section 2 we review the top-level architecture of AstroPIC for operation as a NIR coronagraph with HWO. We show summaries of yield results obtained with the recent Coronagraph Design Survey (CDS) pipeline[5] and the Altruistic Yield Optimization (AYO) design reference mission simulator.[6] These show that a small-scale hybrid AstroPIC already enchances the scientific yield return of HWO and is complementary to traditional coronagraphs. We also show that the full photonic chip AstroPIC approaches 80-85% of the optimal coronagraph yield limits. In Section 3 we provide details of the PIC model which shows that practical PICs implemented with Mach-Zehnder Interferometric (MZI) meshes as proposed here can approach the performance of an optimal coronagraph's theoretical performance with the main limitation being the finite number of modes possible with the practical AstroPIC (and corresponding outer working angle limit). In addition, a PIC model can be used to tolerance the phase shifter elements across the MZI mesh and the effect on coronagraphic performance metrics. In Section 4 we provide an overview of recent key demonstrations at the PIC testbed at Stanford University that show initial experimental results. Additional technical details are in a forthcoming separate publication. Using existing prototype PICs with a 4-element MZI mesh 1e-7 contrast (70 dB) was measured in a 2-channel photonic nulling demonstration; a follow-up result extended the photonic nulling demonstration to 8e-9 contrast (81 dB) by addition of an additional MZI element on the main light path (and providing evidence between increased MZI complexity providing leakage filtering and demonstrated deep photonic nulling). Finally, we show an experiment using a single 4-channel PIC performing coronagraphic nulling and compare this to a pass-through setup (no coronagraph) coupling a free-space beam. As lateral offsets are applied across the input grating couplers, off-axis coronagraphic throughput is shown and compared with on-axis nulling. These demonstrations represent the building blocks of PIC-based coronagraphy. We seek to build on these prototype demonstrations and seek to scale these using a recently submitted Cycle-1 prototype tape-out described in Section 5.

2. ARCHITECTURE

We present here the basic architecture for the AstroPIC coronagraph for HWO as shown in Figure 2. We discuss the basic components of the PIC-based coronagraph and coupling options to the telescope. We outline the particularly useful role a PIC-based coronagraph can serve as NIR-channel coronagraph, but note that it can also be adapted for coverage of additional bands including Visible through appropriate choice of substrate and component maturation.

We use the basic concept of implementing a universal, linear optimal operator through a Mach-Zehnder Interferometric (MZI) mesh.[7] Any coronagraphic operation can be described as a linear transformation between the input field at the coronagraph and its output field at the science detector. This formulation can be used to derive an optimal coronagraph operator as first shown by Guyon et al. 2006[8] and following the theoretical framework in Belikov et al 2021.[2] The optimal coronagraph removes specific low-order modes from the input electric field and has been shown to be broadly compatible with a wide range of telescope apertures whether
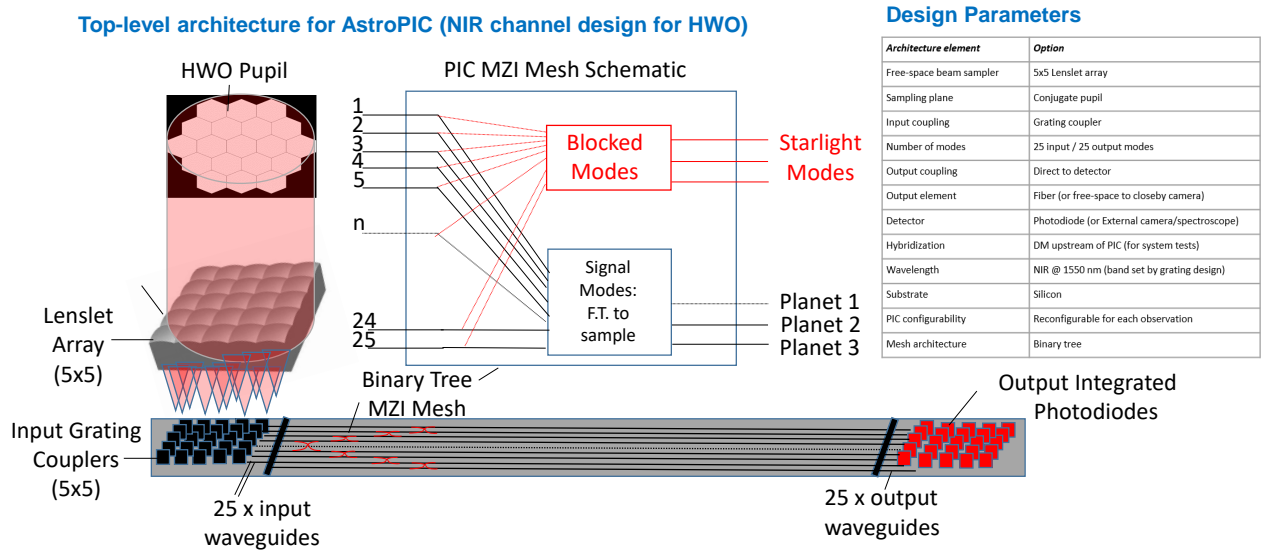
Top-level architecture for AstroPIC (NIR channel design for HWO)

Design Parameters

HWO Pupil

PIC MZI Mesh Schematic

1
2
3
4
5

n

24
25

Blocked Modes — Starlight Modes

Signal Modes: F.T. to sample — Planet 1 / Planet 2 / Planet 3

Lenslet Array (5x5)

Input Grating Couplers (5x5)

Binary Tree MZI Mesh

25 x input waveguides

Output Integrated Photodiodes

25 x output waveguides

Architecture element	Option
Free-space beam sampler	5x5 Lenslet array
Sampling plane	Conjugate pupil
Input coupling	Grating coupler
Number of modes	25 input / 25 output modes
Output coupling	Direct to detector
Output element	Fiber (or free-space to closeby camera)
Detector	Photodiode (or External camera/spectroscope)
Hybridization	DM upstream of PIC (for system tests)
Wavelength	NIR @ 1550 nm (band set by grating design)
Substrate	Silicon
PIC configurability	Reconfigurable for each observation
Mesh architecture	Binary tree

Figure 2: Top-level AstroPIC architecture for HWO as a NIR-channel coronagraph. An image of the telescope pupil plane is discretely sampled by a microlens array determining the number of input modes on the PIC coronagraph. Input grating couplers feed single mode waveguides through to the MZI mesh architecture which performs energy sorting of starlight suppression modes. Additional MZI circuitry can perform an image mode transformation of the exoplanet modes (or alternatively enable complex field measurements). Higher number of blocked starlight modes corresponds to a higher order coronagraph. Shown here is a 25-mode "hybrid" coronagraph architecture which can be scaled to hundreds of modes for a "full photonic chip" coronagraph.

on-axis or off-axis (and spanning all apertures considered for HWO). There is, however, a fundamental trade-off involved in the number of modes removed with increasing robustness to disturbances as higher-order modes are rejected while sacrificing coronagraph inner working angle. In addition, a PIC-based coronagraph is limited by the finite number of channels in which the input light is coupled into and outputted from the PIC, as well as practical manufacturing limitations to the number that can be currently maturely supported. This places constraints on both the outer working angle possible and the specific mesh configuration (through a finite number of MZI elements).

Light can be coupled directly from the HWO pupil into the PIC. An alternative is to re-image the pupil using rejected light from (for example, but not limited to) a focal plane mask in a traditional Lyot-style coronagraph. The PIC can be operated at either the pupil-plane or image-plane with benefits for either configuration –in both cases the basic architecture remains similar. We baseline here a pupil-plane coupling option since it is inherently less chromatic than coupling at an image plane. The telescope pupil is sampled through a lenslet array that matches the number of modes on the PIC input. Microlens arrays are mature elements and provide a high-fill factor, enable robust and high throughput coupling, and can be either externally coupled or manufactured in-situ on the PIC surface through 3D printing (offered by some foundries). Then, to couple light from each individual microlens focus into a specific PIC waveguide, an input grating coupler is used. Grating couplers are traditionally regarded as having lower throughput coupling than other options (e.g., edge couplers or photonic lanterns) but recent designs that maximize the overlap integral with the input electric field now exist that show 90%+ throughputs with bandwidths spanning up to about 50 nm (or 3% at 1.55 um). Input grating couplers can be designed over different bands and central wavelengths using inverse-designed optimization techniques. These were specifically designed for AstroPIC and outlined in Valdez et al 2024[9] producing a well-characterized output
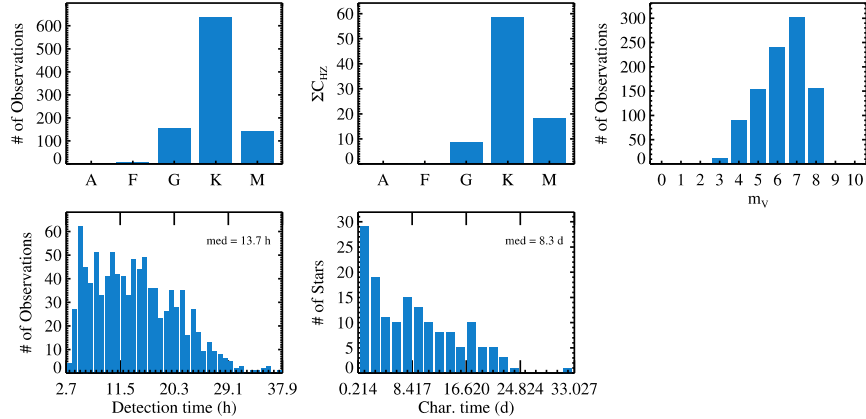
Figure 3: AYO-generated distribution of target stars for a 16-channel, order 4 Hybrid AstroPIC CDS coronagraph operator shows particular sensitivity to K-type stars. This target star preference is complementary to traditional coronagraphs enabled by the small inner working angle of AstroPIC. In addition, the Hybrid AstroPIC can be operated for follow-up NIR characterization at small IWA and can be operated simultaneously for detection and characterization inside the traditional coronagraph's inner working angle.

mode, tuned to the required wavelength range, and potential for polarization-splitting to enable capturing both polarizations in separate waveguides. Finally, input grating couplers have a compact physical footprint which is especially useful for free-space coupling of the beam on the PIC and scaling up the number of modes supported.

After sampling the telescope pupil into a finite number of single-mode waveguides via input grating couplers, a MZI mesh is used to interfere every portion of the pupil to perform coronagraphic nulling. The phase delays at each MZI element are programmed as part of a self-configuration process with modal energy sorting functionality; this concentrates starlight into a limited number of modes. These starlight modes can be directly measured to reconstruct low-order wavefront sensing and control loop to stabilize the optical telescope assembly including direct measurement of the line-of-sight jitter (tip/tilt modes) and other low-order modes. The starlight modes are thus separated from the exoplanet modes and can be considered "blocked"; exoplanet modes are passed through due to their spatial separation and negligible amounts of their energy are coupled into the starlight output modes. Additional PIC circuitry can be included to perform additional signal processing functionality such as image-formation, direct measurement of complex electric fields, or an integrated spectrometer. Finally, at the output of the PIC an integrated photodetector can be included in the PIC for direct measurement at the output waveguide (alternatively, an output grating coupler to an external detector). Different mesh architectures are possible ranging from a compact length binary tree circuit to a highly reconfigurable, fully triangular mesh.

This basic AstroPIC architecture can be scaled across different numbers of input modes. We consider two bounding cases below:

1. "Hybrid" AstroPIC: a 16-channel PIC can be operated together and simultaneously with traditional coronagraph using entirely the rejected starlight inside the traditional coronagraph's inner working angle.

2. "Full photonic chip" AstroPIC: a 400-channel PIC can be operated as a stand-alone channel with reconfiguration of modes tailored to the current observation.

We have generated coronagraph operators using MZI mesh models and using theoretically optimized coronagraphic throughputs assuming a 20% bandwidth consistent with currently demonstrated traditional coronagraphs. We note, however, that leveraging the small mass and volume of the PIC it is possible to use additional PIC MZI meshes and input grating couplers either on the same wafer by splitting different bands off-chip (e.g., with an external dichroic) and coupling each individual band to a different PIC MZI mesh laid out on the same PIC wafer; moreover, it is possible to stack multiple PICs on separate wafers optimized for different wavelengths. Thus, the assumed 20% bandwidth here showed should not be considered a fundamental physical limit

and it possible to extend this by using a stack of PICs matching different channels to simultaneously perform characterization across multiple channels.

A range of coronagraph operators were generated and evaluated through the CDS pipeline (which is described in more detail in a companion paper in the same conference[5]) and their yields computed using the latest version of the AYO DRM). These included both the 16-channel hybrid AstroPIC architecture and the 400-channel full photonic chip AstroPIC evaluated for both order 4 and order 6 starlight suppression and for both the off-axis and on-axis USORT pupils (corresponding to HWO EACs 1 and 3). As part of the standard CDS pipeline output, the coronagraph operator is evaluated for both sensitivities to different types of aberrations and operated through the Altruistic Yield Optimizer (AYO) DRM simulator to estimate its mission lifetime in terms of exoplanet yields characterized and sensitivities to host star astrophysical parameters.

A key finding is that the 16-channel AstroPIC is already scientifically productive generating additional yields (that are "free" as it utilizes starlight that would otherwise be rejected for science) to those obtained using a complementary traditional coronagraph; in addition, we find that hybrid AstroPIC as shown in Figure 3 is showing a unique sensitivity to K-type stars compared to the traditional coronagraph. The preference for K-type stars is seen in the plot of target stype generated by AYO showing a preponderance of K-type stars surveyed on account of the aggressive IWA of the coronagraph and limited by the OWA due to the small number of channel sampling the telescope pupil. We note here that the hybrid architecture of the AstroPIC. A 16-channel AstroPIC is close to current manufacturing capabilities for photonic foundries though technology maturation will be needed to meet key requirements for HWO including contrast, throughput, bandwidth, and robustness. We note that this "hybrid" option of operating in parallel with a traditional coronoagraph is different than others being considered; for example, an alternative architecture also at this conference (see Por et al 2024[10]) hybridizes a PIC coronagraph in sequence with a traditional coronagraph with the goal of relaxing the contrast requirement on both the PIC and the coronagraph.

The full photonic chip 400-channel AstroPIC displays excellent exoplanet chracterization yields that significantly improve beyond a traditional, baseline coronagraph and can reach approximate 80-85% of the optimal coronagraph yield limit as shown in Figure 4. A full PIC-based coronagraph would fully realize the potential of mass and volume miniaturization for the HWO coronagraph instrument; however, PIC technology needs substantial maturation to scale to a large number of modes consistent with a full photonic chip implementation. This requires concerted technology development efforts and investment to demonstrate key coronagraphic requirements.

Finally, we note that either the hybrid or fully photonic options are equally compatible with either on-axis or off-axis HWO apertures. The impact on throughput for optimal mode suppression as implemented with a PIC is highly insensitive to the specific aperture geometry.[2] This offers a path for compatibility with on-axis apertures which have been historically considered to be challenging for coronagraphy.

3. MODEL

In this section we provide a comparison of a MZI-based mesh implementation of an AstroPIC coronagraph operator with an optimal coronagraph operator. This shows that a practical implementation of an optimal coronagraph operator through a PIC recovers some of the key performance characteristics of the optimal coronagraph. We identify the limitation in terms of outer working angle imposed by the finite number of modes across the mesh.

The MZI mesh model is responsible for performing coronagraphic nulling. The mesh model uses full triangular topology following the framework proposed in Miller 2013.[7] The triangular mesh consists of a series of individual MZI nodes, with each node modelled as a 2-input port and 2-output port transforming the electric field at the input to an exit electric field applying the phase delay introduced by phase shifters. A topology of nodes describing the MZI mesh is constructed by generating a matrix of individual nodal phase delays and input/output channel coupling. A separate matrix of individual error terms can also be constructed to tolerance the MZI mesh to individual phase shifter error terms and compute leakages induced by phase shifter inaccuracies (e.g., caused by fabrication errors, temporal thermal shifts at each phase shifter, etc.).

In Figure 5 we show the aperture throughput and radial contrast curves for a finite source for a variety of AstroPIC designs. These include PIC operators for both on-axis and off-axis HWO aperture, with different

	Focal-Plane Coronagraphs			Pupil-Plane Coronagraphs		Hybrid Coronagraphs			Emerging Technologies	
	HLC	VC (monolith)	DMAVC (segmented)	SPC	PIAA (classic)	AAVC	APLC	PAPLC	Full Photonic Chip	Optimal Coro. Limit
Science Yields										
EEC Yield (VIS detections only)	16% (13)	68% (54)	57% (45)	30% (24)	64% (51)	44% (35)	43% (34)	39% (31)	81% (65)	100% (78)
EEC Yield (Detect + orbits + H2O search)	15% (9)	67% (40)	55% (33)	13% (8)	56% (34)	47% (28)	36% (22)	46% (28)	81% (49)	100% (60)
EEC Yield (Detect + orbit + CO2 search)	5% (2)	50% (15)	32% (10)	2% (1)	29% (9)	28% (8)	15% (5)	44% (13)	86% (26)	100% (30)
Total yield of all planet types	13% (170)	62% (838)	47% (635)	12% (157)	45% (605)	43% (582)	25% (333)	40% (543)	65% (875)	100% (1345)
Exposure Times										
Median detection time for blind survey	5.6x (31 hrs)	1.3x (7 hrs)	1.4x (8 hrs)	3.2x (18 hrs)	1.3x (7 hrs)	2.1x (11 hrs)	2.1x (11 hrs)	2.9x (16 hrs)	1.4x (8 hrs)	1x (6 hrs)
Median detection time for fiducial stars	102x (107 hrs)	2.5x (2.6 hrs)	4.0x (4.2 hrs)	310x (325 hrs)	2.5x (2.6 hrs)	8.6x (9.0 hrs)	6.6x (6.9 hrs)	8.5x (8.9 hrs)	3.0x (3.1 hrs)	1x (1.1 hrs)
Median char. time for fiducial stars										

Figure 4: AYO-generated exoplanet yields for a 400-channel, order 4 Full Photonic Chip AstroPIC CDS corona-graph compared to both traditional coronagraphs and an optimal coronagraph. Using the most time-consuming CO2 characterization metric improves yields by a factor of 2-4 compared to traditional coronagraphs, and re-covers 86% of the optimal coronagraph's theoretical yield assuming a 20% band for comparison purposes. In addition, due to its small volume and mass, multiple channels can be added enabling a path to significantly broadening the science bandwidth beyond this nominal level and further increasing exoplanet science yields.

numbers of channels including the 16 and 400 channels point designs discussed in the architecture section, and also both a 4th order and 6th order starlight suppression. Also shown are optimal coronagraph operators at both order 4 and order 6 using the off-axis HWO aperture as a bounding case. A selection of these coronagraph operators were included in the Coronagraph Design Survey, and these were plotted using the same pipeline described in more detail in the corresponding paper.[5] MZI meshes implementing photonic nulling for coronagraphs of order 4 and 6 corresponding to increasing numbers of sorted energy modes being blocked.

The total aperture throughput curves demonstrate nulling and show the inner working angle for different order PIC coronagraphs. These are well matched with expectations from optimal coronagraphs[2] which set a performance bound on both inner working angle and maximum throughput achievable. The primary limitation from a finite number of modes arises in terms of the achievable outer working angle. The finite numbers of modes are responsible for the throughput rollover loss at increasing angular separations and would require additional modes across the PIC to enable a larger field of view for detection and characterization. At a small enough number of modes as illustrated in the 16-channel curves the maximum achievable aperture and inner working throughput is not reached before the outer working angle roll-off occurs. Higher order coronagraphs are naturally more robust to finite stellar diameter but at a finite number of modes this comes at the cost of the smaller field of view and reduced maximum throughput.

The radial contrast curves as a function of angular separation for a finite diameter source also illustrates the improvement in robustness for a higher-order coronagraph and performance improvements possible with higher numbers of modes. The finite star used here has a diameter of 0.05 λ/D (without using applying limb darkening)– more than 80% of the current HWO target list would be inside this stellar diameter.[11] Meanwhile point sources are optimally suppressed by the PIC coronagraph. The 6th order PIC operator shows excellent robustness to stellar diameter while the 4th order PIC operators as described in the yield results in the previous section generate high yields and their small inner working angles and high throughput makes them excellent at characterizing smaller diameter stars.

We also note here that in terms of both sensitivity to a finite source and throughput, the AstroPIC operators have similar performance both for on-axis and off-axis HWO apertures.

These model comparisons demonstrate that optimal coronagraph performance is recovered with a practical MZI mesh model with a finite number of nodes across the mesh. The main limitation arises in terms of the outer working angle. This model enables tolerancing fabrication errors across individual phase delay terms; this will enable placing component manufacturing tolerances for the critical phase delay elements and performing in-depth trades on the achieved photonic nulling. Propagation losses and coupling loses are implemented as parametric
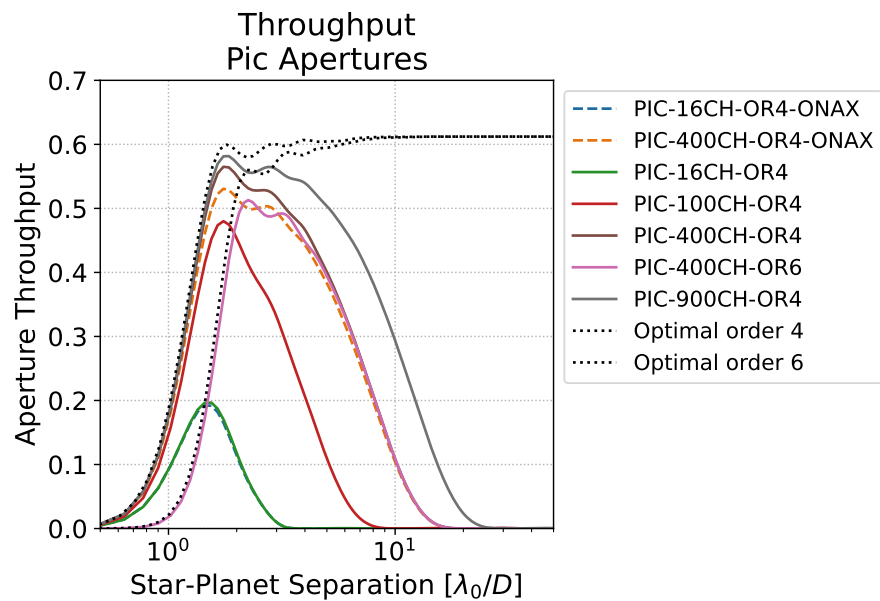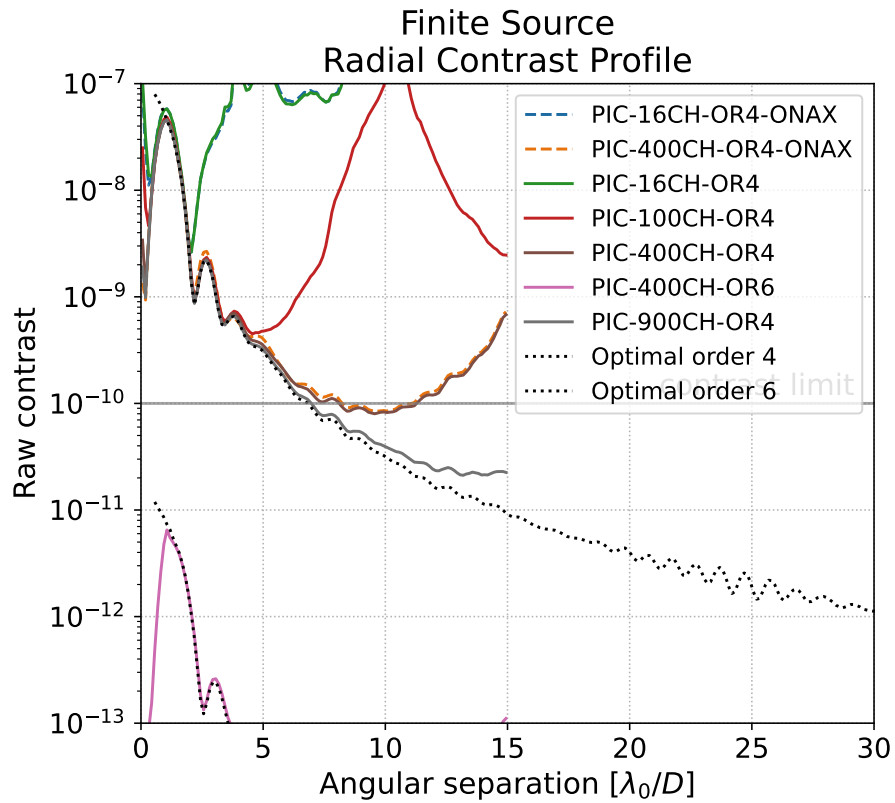
Figure 5: Contrast and throughput curves for different AstroPIC point designs with varying numbers of channel, starlight suppression order for both off-axis and on-axis HWO apertures and comparison with the optimal coronagraph boundary. Top: contrast curves for finite star of 0.05 λ/D diameter star at 20% bandwidth. Bottom: corresponding throughput curves as a function of angular separation
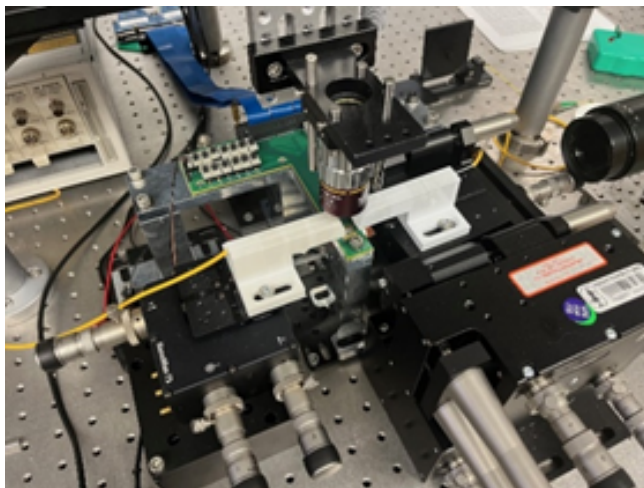
Figure 6: Photonic integrated circuit test stand at Stanford University utilized to perform photonic nulling and free-space coupling demonstrations. The test stand consists of an aluminum mount on which the PIC and its PCB packaging are setup with micropositioning stages at both PIC input and output, controllers for setting thermal phase shifters and data acquisition, as well as two cameras for top-down and side visual inspection.

settings at this point, with plans to add higher-level fidelity. The ability to recover near-optimal performance limited by a finite number of modes is also discussed at this conference elsewhere.[12]

4. EXPERIMENTS

In this section, we provide an overview of a series of experiments designed to demonstrate the basic coronagraphic functionality of a PIC-based photonic nuller. These experiments have been selected to cover the fundamental coronagraphic nulling operation as well as measurement of coronagraphic throughput through free-space coupling as a function of source offset. These experiments used existing MZI-mesh prototypes that were originally manufactured for other applications[13] but were re-configured and utilized for these coronagraphic functionality demonstrations. The ability to re-configure an existing mesh for new applications shows the flexibility and programmability potential of general MZI meshes. Two experiments focused on achieving deep photonic nulling across a single output channel and achieved contrasts by over two orders of magnitude than has been demonstrate to date in the literature[14] with performance improvements possible through the usage of additional MZI elements along the optical path and a careful configuration procedure that minimizes off-axis light paths to minimize leakage. The final experiment demonstrated basic free-space coupling functionality with the potential to substantially optimize end-to-end throughput using the input coupling architecture previously described in Section 2.

These demonstrations were carried out in Stanford University's Solgaard Lab within the Electrical & Computer Engineering Department shown in Figure 6. The PIC test stand consists of an aluminum mount on which the PIC is set onto a printed cicruit board that provides packaging and interfacing through a data acquisition controller and thermal controller to a control computer. Micropositioners are used at both the PIC input and the output; the laser is through a single-mode fiber (or fiber array) at the input. At the output a 6-axis stage is used to perform PIC measurements by coupling a single-mode fiber to a detector by measuring PIC output channels. Two microscopes are available for inspection of the PIC with both top and side-views.

4.1 Photonic nulling at 1e-7 contrast (70 dB), single-channel

The first experiment was carried out using a simple 4-MZI element mesh circuit which was setup in two different configurations as shown in Figure 7. In one configuration, the phase shifters on the 4-MZI elements are configured to minimize the power output from 2-input ports; in the second configuration, the phase shifters are set to maximize the optical power at the same output channel. A laser is scanned over a 10-nm narrowband channel and contrast is measured between the two configurations achieving a ratio of 1e-7 (or 70dB). This experiment
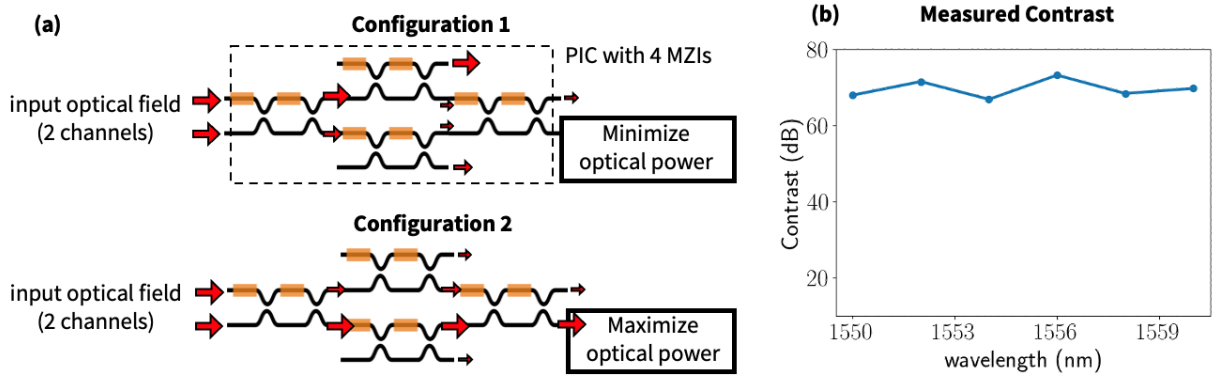
Figure 7: (a) Dual configuration of 4-MZI mesh configured for minimizing and maximizing power at an output channel of the PIC. (b) Measured contrast ratio across a 10 nm narrowband showing a demonstrated 1e-7 contrast level (or 70 dB) at the output channel

represents a factor of 10x improvement over the previously best previously demonstrated contrast in the literature.[14] Providing further support of the contrast limit for this architecture, a similar contrast level was also reported using a similar 4-MZI architecture at this same conference[15] although manufactured using a different commercial foundry. The end-to-end measured throughput is approximately 10% and dominated by losses from using both a standard, foundry-provided input and output grating coupler with approximately 30% coupling efficiency, while silicon substrate absorption losses at 1.55 um are approximately 20% per cm of propagation distance. For high-throughput demonstrations switching to a silicon nitride substrate would reduce propagation losses by a factor of 10 (approximately 2% per cm of propagation distance) while manufacturing custom-designed grating couplers[9] enables reaching the high-efficiency couplings designed for better than 90% throughput.

4.2 Photonic nulling at 8e-9 contrast (81 dB), single-channel

The goal of the follow-up experiment is to both stabilize and obtain deeper photonic nulling. This is achieved by adopting a Perfect MZI architecture (PMZI) which enables fine-tuning imperfections as proposed in Miller 2015. In this experiment, the Perfect MZI architecture is used to improve photonic nulling by an additional order of magnitude across a single channel to 7.9e-9 (81 dB) contrast using an iterative tuning procedure. The key experimental details, a detailed PIC tuning procedure, and measured data will be reported in a separate technical publication in Valdez et al 2024b.[16]

An important architectural insight from this experiment is that there is a trade-off between circuit complexity with additional MZI elements required to enable the deepest nulls and the scalability of the PIC circuit within a finite footprint. This informs our dedicated Cycle-1 design described in more detail in Section 5. In addition, the PIC tuning procedure can be used dynamically in a similar way to wavefront sensing and control functionality in traditional coronagraphs to maximize energy in the starlight modes and enhance contrast in exoplanet signal modes.

4.3 Free-space coupling, four-channel

The final experiment we report on demonstrated coronagraphic throughput and nulling using a simple four-channel configuration as shown below in Figure 8. In this experiment a Gaussian beam from a fiber is illuminating 4 input grating couplers, and the Gaussian beam is laterally translated in one-direction as indicated. The MZI mesh is configured in two different configuration: (1) as a simple pass-through circuit demonstrating the lack of coronagraphic supression while (2) minimizes starlight into a single channel-1.
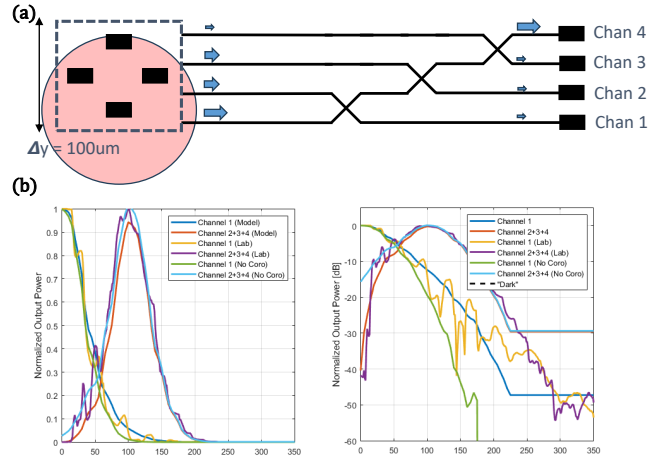
Figure 8: (a) Four-channel configuration setup to minimize output in a , (b) PMZI circuit portion of PIC layout used for experiments, and (c) Time-series of output channel suppression as individual phase shifters are sequentially tuned to enable the energy minimization configuration.
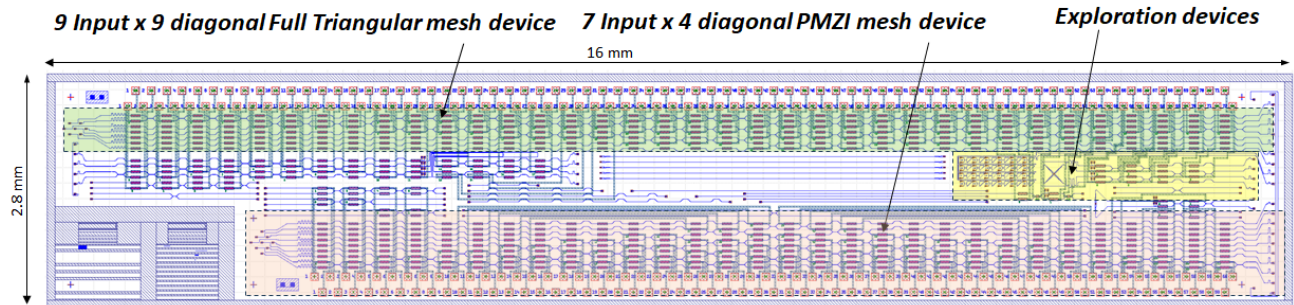

Figure 9: Overview of the AstroPIC Cycle 1 PIC which includes multiple devices: (1) a full triangular mesh featuring 9 input grating couplers arranged in a 3x3 configuration and 9 linear output grating couplers for off-PIC measurement, (2) a 7-input and 4-diagonal Perfect MZI mesh device, and (3) a series of exploratory devices including parametric sweeps of directional couplers for optimizing bandwidths and polarization splitting input couplers.

The plot of coronagraphic throughput measurements across all four channels as a function of later offsets shows a comparison between the Stanford experimental data and the Ames coronagraph model. In the no-coronagraph case, the beam is simply passed through. However, in the coronagraphic case, the on-axis mode mode is blocked and as the offset increases the coronagraph transmission becomes apparent. This represents a measurement of coronagraphic throughput when the beam is moved laterally (off-axis) while on-axis there is coronagraphic suppression occurring at the 1e-4 contrast level (40 dB).

This demonstration also illustrates the additional complexity associated with scaling to multiple modes when additional channels are introduced. There is a single MZI element here between individual input and output channels so the achievable contrast is similar to that achieved in previous demonstration after tuning only 1 phase shifter in the optical path. However, it demonstrates the key coronagraphic property of blocking on-axis light in a single piston channel while passing through off-axis light in the remaining 3 channels.

5. CYCLE-1 TAPE-OUT

In this section, we provide an overview of the key design features of the Cycle-1 AstroPIC layout, which was recently submitted to a commercial photonic foundry (Advanced Microfoundries) completing the tape-out. This

Cycle-1 design leverages heritage with this commercial foundry from the initial prototypes used for the experiments described in Section 4. We expect to receive the device in the fall to begin photonic nulling a second round of experimentation and demonstrate additional PIC-based coronagraphic capabilities.

The Cycle-1 AstroPIC device is shown in Figure 9. Two main coronagraphic devices are featured on this layout as indicated. The size of the PIC is set by the reticle size used by the foundry (2.8 mm x 16 mm) which sets a limit on the number of bond pads that can be easily included in an unfolded layout configuration and sets the upper limit of number of modes in this design. This device is using the standard silicon substrate process and features no active elements. Standard input grating coupler elements are used, directional couplers tuned to 1.55 um, and two main mesh topologies. This is a passive device without integrated photodetector, and grating couplers are used to couple to a detector outside the device (similar to the existing prototype).

The first device is a full triangular mesh featuring 9 input modes and 9 diagonals. The 9 input modes use standard grating coupler elements across both inputs and output (and which we expect to be the main throughput limiter). The input grating couplers are setup in a 3x3 configuration to enable free-space beam coupling using an external microlens array. The number of bond pads available limit the number of phase shifters and set the limit to the number of possible modes across the MZI mesh. This device will allow an expanded version of the the free-space coupling demonstration enabling deeper contrasts with higher numbers of modes and supporting input with a high-fill factor microlens array and will allow measurements of coronagraphic throughput, inner working angle and outer working angle.

The second device features a 7 input and 4 diagonal PMZI mesh.With each PMZI element consisting of two sequential MZIs we expect to enable deeper suppression with the goal of reaching 1e-9 contrast levels, and test scaling across multiple input channels with the capability of reducing cross-channel leakage. To enable the PMZI device, we double the number of phase shifters compared to a comparable triangular mesh hence the lower number of modes and diagonals on this device. However, it will enable the deepest contrast demonstrations (using fewer input modes) and provide a path for scaling at deep contrasts with more modes.

Finally, we have a number of exploratory devices that perform parametric sweeps on directional couplers to enable future broadband tests. We have a couple of custom designed input grating couplers that allow separation of bands and polarization on the PIC. This will provide a possible path to performing, for example, dual polarization demonstrations on a single chip. These exploratory devices will allow us to tune the specifications of a future Cycle-2 device operating at different bands, and provide measurable verification of as-manufactured component specifications and performance.

6. CONCLUSIONS

In this paper, we have provided an overview and progress of the AstroPIC project. This project aims to build a photonic nuller using a PIC-based architecture to miniaturize coronagraphic instrumentation and improve coronagraphic efficiency and robustness. We have described the top-level architecture of AstroPIC and its synergy with the NIR channel for HWO with the potential to be used in either a hybrid configuration with a traditional coronagraph enabling additional, free science yields using otherwise rejected starlight. We have also described a full photonic chip AstroPIC that would require concerted technology development to scale to sufficient numbers of modes and meet coronagraphic performance requirements, but could fully realize the miniaturization potential of PICs for HWO. Although there is natural synergy and greater maturity to date with a NIR channel, we emphasize PICs can also be built on a substrate (e.g., silicon nitride) for a visible channel.

We have shown how a practical PIC implementation using a MZI mesh recovers an optimal coronagraph but whose outer working angle is limited by the finite number of modes through a MZI mesh model.

We have summarized three recent experiments that re-purposed general MZI-meshes on existing PIC devices and have demonstrated key coronagraphic functionality. The details of these experiments will be forthcoming in a separate technical publication,[16] and report here at top-level we have shown single-channel suppression culminating in a 7.9e-9 contrast – this is deeper by two orders of magnitude than previously demonstrated in the literature[14] and more details and insights in the trade-off between mesh complexity and nulling will be discussed in an upcoming publication.[16] We have also shown coronagraphic nulling as a function of lateral offsets blocking

on-axis light and enabling coronagraphic throughput of off-axis light, with good agreement between experiment and model.

Finally, we have provided an overview of the custom-designed Cycle-1 AstroPIC device that was recently submitted to the foundry tape-out. Informed by the experiments overviewed here, we expect to be able to demonstrate deeper contrasts potentially reaching 1e-9 contrast, scale to multiple channels, and demonstrate free-space coupling in upcoming experiments.

ACKNOWLEDGMENTS

REFERENCES

[1] National Academies of Sciences, Engineering, and Medicine 2021, *Pathways to Discovery in Astronomy and Astrophysics for the 2020s*, The National Academies Press, Washington,, DC.

[2] R. Belikov, D. Sirbu, J. Jewell, O. Guyon, and C. Stark, "Theoretical performance limits for coronagraphs on obstructed and unobstructed apertures: How much can current designs be improved?," *Proc. SPIE* **11823**, 2021.

[3] "Astrophyics directory technology gap list," *White Paper* , 2022. `https://apd440.gsfc.nasa.gov/tech_gap_priorities.html`.

[4] N. Jovanovic *et al.*, "2023 Astrophotonics Roadmap: pathways to realizing multi-functional integrated astrophotonic instruments," *J. Phys. Photonics* **5**, 2021.

[5] R. Belikov *et al.*, "Coronagraph design survey for future exoplanet direct imaging space missions," *Proc. SPIE* **13092**, 2024.

[6] C. Stark *et al.*, "The ExoEarth Yield Landscape for Future Direct Imaging Space Telescopes," *JATIS* **5**(2), 2019.

[7] D.A.B. Miller, "Self-configuring universal linear optical component," *Phot. Res.* **1**, 2013.

[8] O. Guyon, E. Pluzhnik, M. Kuchner, B. Collins, and S. Ridgway, "Theoretical limits on extrasolar terrestrial planet detection with coronagraphs," *ApJS* **167**, 2006.

[9] C. Valdez, S. Pai, P. Broaddus, and O. Solgaard, "High-efficiency vertically emitting coupler facilitated by three wave interaction gratings," *Opt. Lett.* **49**, 2024.

[10] E. Por *et al.*, "A hybrid coronagraphic approach using photonic integrated circuits and bulk optics coronagraphs," *Proc. SPIE* **13092**, 2024.

[11] E. Mamajek and K. Stapelfeldt, "NASA Exoplanet Exploration Program (ExEP) Mission Star List for the Habitable Worlds Observatory," *arXiv:2402.12414* , 2024. NASA Exoplanet Archive at NExSCI `https://exoplanetarchive.ipac.caltech.edu/cgi-bin/TblView/nph-tblView?app=ExoTbls&config=DI_STARS_EXEP`.

[12] O. Guyon *et al.*, "Self-calibrating photonic nulling systems for exoplanet imaging and spectroscopy," *Proc. SPIE* **13092**, 2024.

[13] S. Pai, Z. Sun, *et al.*, "Experimentally realized in situ backpropagation for deep learning in photonic neural networks," *Science* **380**, 2023.

[14] C. Wilkes *et al.*, "60 dB high-extinction auto-configured Mach-Zehnder Interferometer," *Opt. Lett.* **41**, 2016.

[15] J. Jewell *et al.*, "A photonic coronagraph architecture achieving theoretical near ideal performance," *Proc. SPIE* **13092**, 2024.

[16] C. Valdez *et al.*, "Leveraging Architectural Redundancy for High Contrast Nulling with Mach-Zehnder Interferometer Meshes," *Manuscript in Preparation, Electrical Engineering, Stanford University* **380**, 2025.